Revista Mexicana de Astronomía y Astrofísica, **40**, 181–191 (2004)

DETERMINATION OF STELLAR ATMOSPHERIC PARAMETERS FROM THE NEAR-IR REGION

R. Molina[1] and J. Stock[2]

Received 2004 March 15; accepted 2004 June 29

RESUMEN

Se analiza una muestra de 211 estrellas gigantes con tipos espectrales K y M cuyos pseudo anchos equivalentes fueron medidos y sus parámetros atmosféricos estelares previamente identificados. Los espectros de estas estrellas provienen de una biblioteca estelar y fueron tomados con el telescopio Coudé del Kitt Peak National Observatory, a una resolución de ~ 1 Å FWHM; abarcan un intervalo de longitud de onda de $\lambda\lambda$3460–9460 Å. Se aplica un conjunto de polinomios de primer y segundo orden que involucra una, dos o tres variables independientes el cual permite estimar la precisión en la temperatura efectiva $T_{\rm eff}$, la gravedad superficial $\log g$ y la metalicidad [Fe/H] en términos de medidas de los anchos equivalentes de siete líneas de absorción presentes en la región infrarroja cercana $\lambda\lambda$5400–9500 Å. Los resultados obtenidos en los ajustes lineales con tres variables independientes a los tres parámetros atmosféricos fundamentales alcanzan residuos promedios de (149±15) K, (0.26±0.02) dex, (0.12±0.02) dex, mientras los ajustes cuadráticos tienen residuos promedios de (146±16) K, (0.25±0.02) dex, (0.12±0.02) dex, respectivamente. Se observa de ambos resultados que el uso de polinomios de orden superior no ofrece ventajas en los residuos promedio respecto a las soluciones lineales. El procedimiento empleado sigue el método de Stock & Stock (1999).

ABSTRACT

A sample of 211 giant stars with spectral types K and M has been analyzed, for which pseudo-equivalent widths were measured and stellar atmospheric parameters were previously identified. The spectra of these stars have been taken from a stellar library observed with the Coudé telescope at the Kitt Peak National Observatory, with a resolution of ~ 1 Å FWHM and covering a spectral region of $\lambda\lambda$3460–9460 Å. A set of first and second order polynomials is applied, which involves one, two, or three independent variables and allows us to estimate the precision in the effective temperature $T_{\rm eff}$, the surface gravity, $\log g$ and the metallicity [Fe/H] in terms of the pseudo-equivalent widths of seven absorption features in the near IR regions $\lambda\lambda$5400–9500 Å. The results obtained from linear fittings with three independent variables to the three fundamental atmospheric parameters attain residual averages of (149±15) K, (0.26±0,02) dex, (0.12±0.02) dex, while the quadratic fittings attain residual averages of (146±16) K, (0.25±0.02) dex, (0.12±0.02) dex, respectively. It is observed from both results that using higher order polynomials does not improve the residual averages with respect to those obtained from linear fittings. The procedure performed in this work follows the Stock & Stock method (1999).

Key Words: **STARS: ABUNDANCES — STARS: ATMOSPHERES**

[1]Universidad Nacional Experimental del Táchira, Venezuela.
[2]Centro de Investigaciones de Astronomía, Mérida, Venezuela.

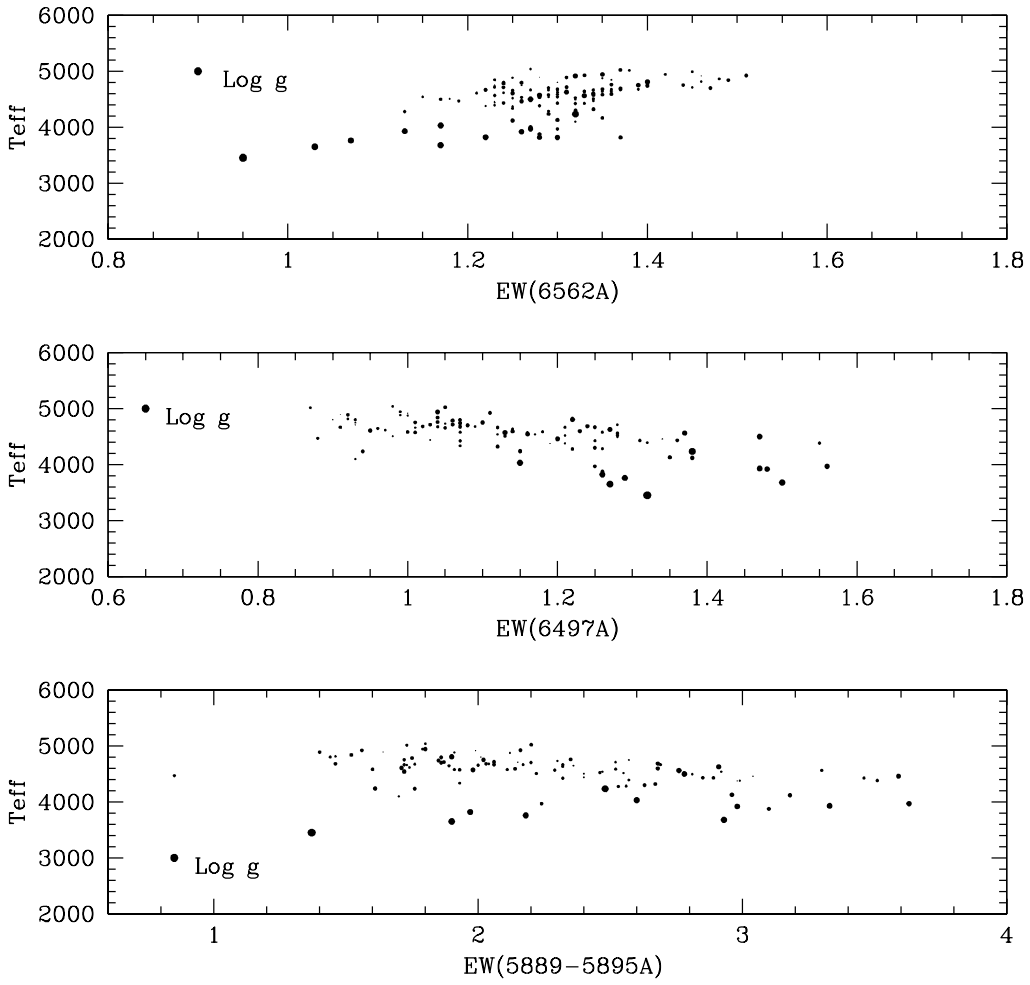

Fig. 1. Relation between the pseudo-equivalent widths in Angstroms and the effective temperature for three different lines. The size of the symbols represents the surface gravity of the objects.

1. INTRODUCTION

In the near-IR spectral region, the Ca II triplet (8498, 8542, 8662 Å) has been one of the spectral absorption features most widely used in the determination of the fundamental atmospheric parameters $T_{\rm eff}$, log g, and [Fe/H]. Several researchers have used this prominent feature with this intention, among others Jones, Alloin, & Jones (1984); Carter, Visvanathan, & Pickles (1986); Alloin & Bica (1989); Diaz, Terlevich, & Terlevich (1989); Zhou (1991); Mallik (1994); Cenarro et al. (2001a, 2001b, 2002). However, there exist some contradictions between the different authors with respect to the dependence of the Ca II triplet on the three fundamental atmospheric parameters. Cenarro et al. (2002) indicates that these discrepancies arise mainly because of the lack of a wide database with a homogenous range in its fundamental parameters and of a proper definition of the spectral indices used. In order to clarify these discordant results, we use a new homogenous stellar spectra library that contains 706 stars with a resolution of 1.5 Å FWHM and covers a spectral region of $\lambda\lambda$ 8348–9020 Å. The Ca II triplet behavior in cool stars is analyzed as well as its overlap with the hydrogen Paschen lines in hot stars by constructing two spectral indices CaT and PaT, respectively. Moreover, we construct a third spectral index CaT* as a pure Ca II indicator, that is, we eliminate the Paschen line contamination. We apply empirical fittings to functions that allow to describe the behavior of the three spectral indices in terms of the fundamental atmospheric parameters, so that these functions can later be implemented in evolutionary

TABLE 1

POINTS THAT DEFINE THE LOCAL CONTINUUM
FOR EACH IDENTIFIED LINE

Lines	L_1 (Å)	L_2 (Å)	P_1 (Å)	P_2 (Å)	L_3 (Å)	L_4 (Å)	Element
1	5860.2	5864.1	5861.0	5908.0	5907.5	5910.6	Na I
2	6484.3	6485.5	6484.2	6503.6	6502.8	6504.7	Blend
3	6549.8	6554.1	6551.7	6576.8	6575.0	6580.2	Hα
4	8490.9	8493.1	8492.3	8508.1	8507.5	8510.1	Ca II
5	8528.8	8537.5	8536.1	8551.5	8550.5	8554.7	Ca II
6	8658.1	8665.6	8660.2	8669.3	8666.0	8680.4	Ca II
7	8448.1	8454.7	8450.4	8736.5	8730.4	8740.6	Triplet

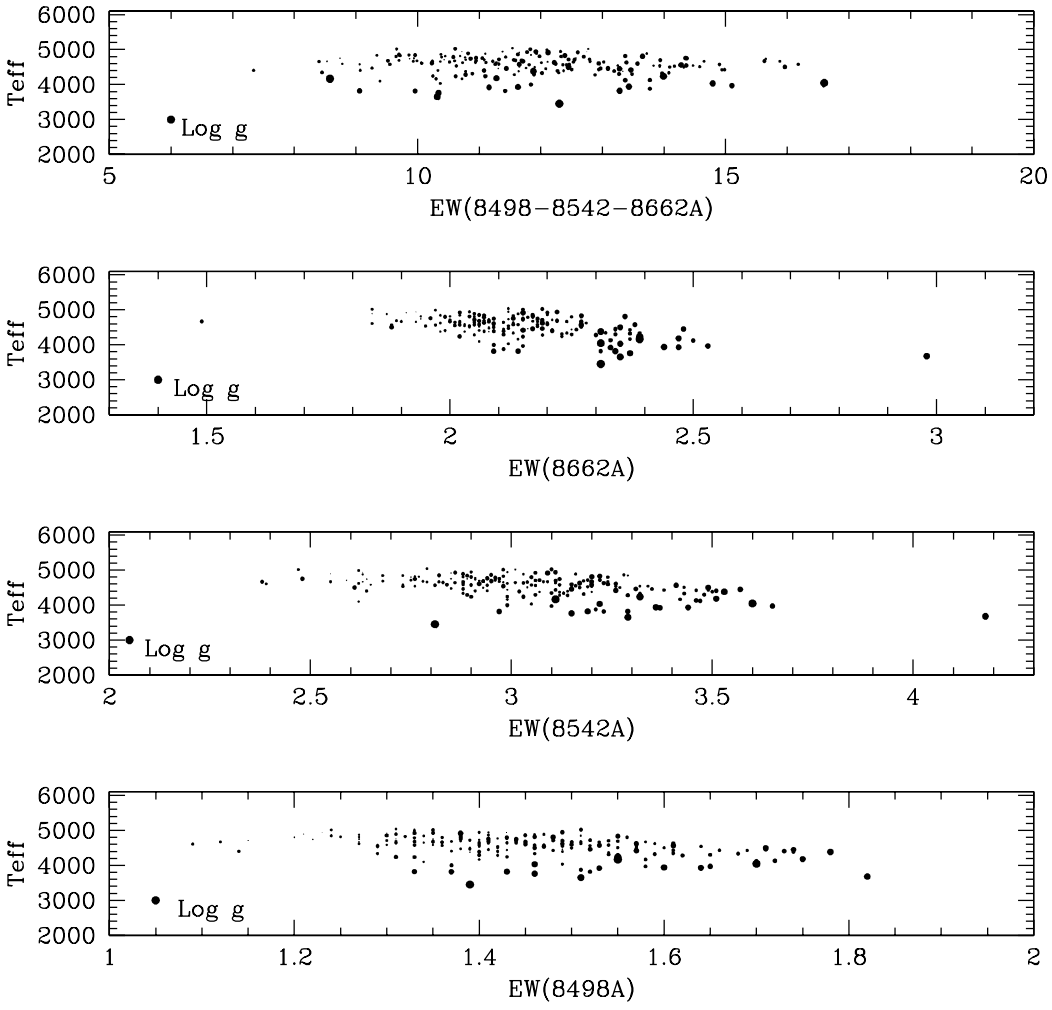

Fig. 2. Relation between the pseudo-equivalent widths in Angstroms and the effective temperature for Ca II triplet lines. The size of the symbols represents the surface gravity of the objects.

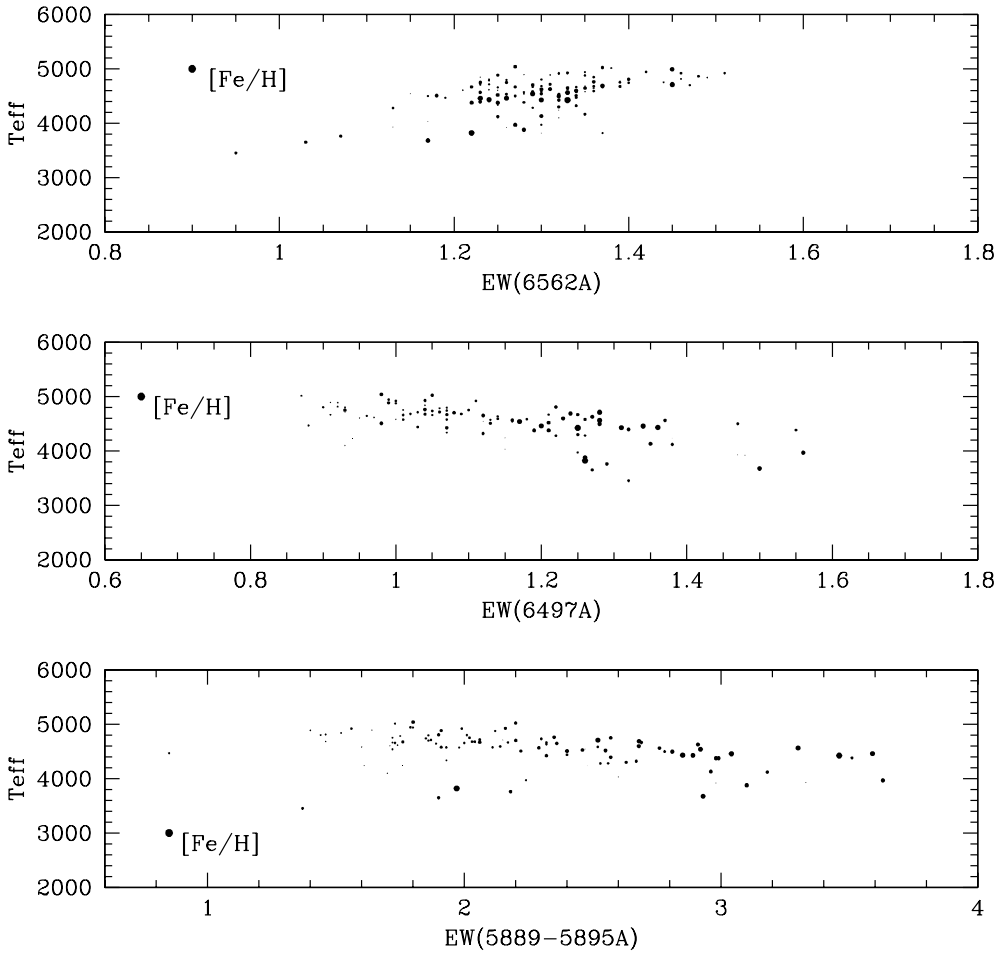

Fig. 3. Relation between the pseudo-equivalent widths in Angstroms and the effective temperature for three different lines. The size of the symbols represents the metallicity of the objects.

models of stellar populations synthesis (Vazdekis et al. 2003). We study the behavior of the spectral indices with the three atmospheric parameters, and find in a general way that: (*i*) for hot stars ($T_{\rm eff} > 6300$ K) and cool stars ($T_{\rm eff} < 3877$ K) there exists a complex dependence of the Ca II triplet on the effective temperature and metallicity, and (*ii*) for stars that cover a range in effective temperature ($3877 \leq T_{\rm eff} \leq 6300$ K), the Ca II triplet presents sensitivity to the three fundamental atmospheric parameters. In this work, we study the behavior of the individual lines and the complete feature of the Ca II triplet absorption line, as well as the complete NaI doublet (5888–5895 Å), a blend at 6497 Å, and the line Hα (6562 Å) as a function of the three fundamental atmospheric parameters. In the analysis, pseudo equivalent widths of all mentioned absorption lines are measured for a sample of 211 giant stars with spectral types K-M, which includes a range in effective temperature between $3400 \leq T_{\rm eff} \leq 5100$ K. The main purpose of this work is to recover $T_{\rm eff}$, log g, and [Fe/H] by the application of empirical fittings of first and second order polynomials where the pseudo-equivalent widths are used as independent variables. A set of $C_{n,m}$ combinations appears when one, two, or three independent variables are used, which allows us to estimate the mean error in each fitting. The technique used in this work follows the procedure used by Stock & Stock (1999). It is important to remark that the sample of stars in this work is restricted to those with an error on the parallax less than, or equal to, 20%. The reason is that this sample was constructed initially to recover the observable parameters M_V and (B-V) with this technique and the results were compared to those obtained by Artificial Neural Network (ANN). Thus, a wider study in which we will include stars of luminosities classes III, IV, and V is being performed at the moment.

TABLE 2

RESULTS OF THE RESIDUAL AVERAGES OF THE TOTAL COMBINATIONS[a]

Independent Variables	Mean Error, σ Linear fit	Mean Error, σ Quadratic fit
	$T_{\rm eff} \pm \sigma_{T_{\rm eff}}$	$T_{\rm eff} \pm \sigma_{T_{\rm eff}}$
1	198 ± 34	184 ± 18
2	167 ± 25	164 ± 17
3	149 ± 15	146 ± 16
4	...	51 ± 7
	$\log g \pm \sigma_{\log g}$	$\log g \pm \sigma_{\log g}$
1	0.27 ± 0.02	0.28 ± 0.03
2	0.27 ± 0.03	0.27 ± 0.03
3	0.26 ± 0.02	0.25 ± 0.02
4	...	0.24 ± 0.01
	$_{[Fe/H]} \pm \sigma_{[Fe/H]}$	$_{[Fe/H]} \pm \sigma_{[Fe/H]}$
1	0.15 ± 0.01	0.14 ± 0.02
2	0.13 ± 0.02	0.13 ± 0.02
3	0.12 ± 0.02	0.12 ± 0.02
4	...	0.12 ± 0.02

[a]Performed by linear and quadratic solutions.

2. DATABASE

For this work, a stellar spectra library that covers a wide range in $T_{\rm eff}$, log g, and [Fe/H] is used. The stars were selected from a large homogenous sample and their atmospheric parameters were obtained from diverse sources of high resolution spectra (see § 3 and Table 3 in Valdes et al. 2004). The complete sample contains digitized spectra of 1301 stars, which were taken with the Coudé telescope of the Kitt Peak National Observatory. The spectra have a resolution of $\sim$ 1 Å FWHM, at an original dispersion of 0.44 Å/pixel and cover a wavelength range of $\lambda\lambda$3460–9464 Å. A detailed explanation of this stellar library is given in Valdes et al. (2004). From the total spectra contained in the library, a sample of 211 giant stars with spectral types K-M was analyzed, and the pseudo-equivalent widths of the seven absorption features were calculated. To measure such pseudo-equivalent widths, a pseudo continuum or continuum is constructed taking two points (L1, L2 and L3, L4) separated by a small range of wavelength and positioned to both sides of the absorption line. The average values (P1, P2) in both intervals determine the local continuum through a straight line. A numerical integration determines the total area measured. Table 1 shows the different points that limit the local continuum for each identified line. This procedure is used by Worthey et al. (1994).

3. METHODOLOGY

Considering the pseudo-equivalent widths, we applied a set of first and second order polynomials with the purpose of generating empirical functions that allow us to deduce $T_{\rm eff}$, log g, and [Fe/H]. These Ew's are introduced as independent variables in polynomial fittings. The best constants involved in each polynomial are obtained from an algorithm that uses a least-squares method. This algorithm discards all those residuals greater than 2.5σ and the process is repeated until no discards appear. A set of $_{Cn,m}$ = n!/m!(n−m)! combinations appears when one, two or three independent variables are used. In fact, we achieved 7, 21, and 35 combinations, respectively. We obtained individual residuals for the different combinations performed in the recovery of the three fundamental atmospheric parameters. Table 2 shows the residual averages of all the possible combinations for the three fundamental atmospheric parameters, using one, two and three independent variables. On the

other hand, the color (B−V) is used as a fourth independent variable with the purpose of improving the empirical functions that allow us to recover the three fundamental atmospheric parameters. Because of the restriction of the star sample to an error in trigonometric parallax less than, or equal to, 20%, the interstellar reddening effect is neglected. The residual averages can be seen in Table 2 only for those fittings that involve quadratic polynomials. Table 3 shows all the linear polynomial coefficients obtained for $T_{\rm eff}$, log g, and [Fe/H] from the algorithm that uses the least-squares method and three independent variables. The columns L_1, L_2, and L_3 correspond to combinations performed with the independent variables. The columns a_{0i} represent the coefficients of the polynomials. The two following columns represent the number of stars used for the fitting and left out of it, respectively. The last column represents the residuals in each fitting for the three fundamental atmospheric parameters.

4. EXPERIMENTAL RESULTS

4.1. *Effective Temperature*

A qualitative analysis of the relation between the seven measured absorption features and the effective temperature can be seen in Figures 1 and 2. The size of the points represents the surface gravity variation for the giant stars studied. It is observed in both figures that there exists a dependence of all the absorption features on the effective temperature, in contrast with results of Jones et al. (1984) and Díaz et al. (1989). We can notice from Table 2 that the increase of the number of independent variables leads to an improvement of the residual averages of the effective temperature. The residuals considerably decrease when we make use of the color index (B-V) as a fourth independent variable. It is well known that the color index is a good indicator of the effective temperature, being less affected by the overlapping of lines that depends on the metal abundance (Díaz et al. 1989). The best fitting that recovers the effective temperature within a range of 3400 $\leq T_{\rm eff} \leq$ 5100 K, is represented by a second order polynomial having the following form

$$\begin{aligned} T_{\rm eff} = & -3368 + 557 * EW_1 + 12427 * EW_3 \\ & - 664 * EW_6 - 470 * EW_1 * EW_3 \\ & + 31 * EW_1 * EW_6 + 967 * EW_3 * EW_6 \\ & - 35 * EW_1^2 - 4708 * EW_3^2 - 289 * EW_6^2 \ , \end{aligned}$$

where EW_1, EW_3, EW_6 correspond to the combinations 1 3 6, and the residual attains a value of 115 K. The range of the residuals of $T_{\rm eff}$ obtained for the linear solutions when we use one, two and three independent variables attains the values $\sigma T_{\rm eff} = 159 - 264$ K, $\sigma T_{\rm eff} = 130 - 241$ K, $\sigma T_{\rm eff} = 125 - 193$ K, while using least-square solutions we find $\sigma T_{\rm eff} = 163 - 218$ K, $\sigma T_{\rm eff} = 128 - 194$ K, $\sigma T_{\rm eff} = 115 - 181$ K, respectively.

4.2. *Surface Gravities*

Returning to the qualitative analysis of Figures 1 and 2, the size of the points is designed to represent the surface gravity. The large points represent stars with a greater gravity and the small points represent stars with smaller gravity. It is observed for all the correlations that stars with a greater gravity are clearly separated from those of smaller gravity. This allows us to state that either the Ca II triplet or the other absorption features are sensitive to stellar gravity. The behavior observed agrees with that indicated by Cenarro et al. (2002), who state that the Ca II triplet is more sensitive to gravity in giant and supergiant stars than in dwarf stars. The Ca II triplet dependence on the surface gravity has been studied by different researchers (see Table 2, Cenarro et al. 2002), the dependence of the blend at 6497 Å on the stellar luminosity has been studied by Malyuto & Schmidt-Kaler (1999). Also well known is the dependence of the NaI doublet on surface gravity (Alloin & Bica 1989; Zhou 1991). In the same way, the Hα line is also sensitive to surface gravity, as indicated by Weaver & Torres-Dodgen's (1995) for A-type stars. The best fitting that recovers the surface gravity within a range of $0.9 \leq \log g \leq 3.4$, involves a second order polynomial, that is,

$$\begin{aligned}\log g =& 10.67 + 2.04 * EW_1 - 14.32 * EW_4 \\ &+ 0.09 * EW_7 - 1.71 * EW_1 * EW_4 \\ &+ 0.02 * EW_1 * EW_7 - 0.33 * EW_4 * EW_7 \\ &+ 0.09 * EW_1^2 + 7.16 * EW_4^2 + 0.01 * EW_7^2 \ ,\end{aligned}$$

where EW_1, EW_4, and EW_7 correspond to the combinations 1 4 7 and the residual attains a value of 0.20 dex. The range of the residuals of log g obtained for the linear solutions when we use one, two and three independent variables attains the values σ log $g = 0.24 - 0.31$ dex, σ *log* $g = 0.23 - 0.33$ dex, σ log $g = 0.22 - 0.31$ dex, while using least-squares solutions we find σ log $g = 0.24 - 0.30$ dex, σ log $g = 0.22 - 0.33$ dex, σ log $g = 0.20 - 0.30$, respectively.

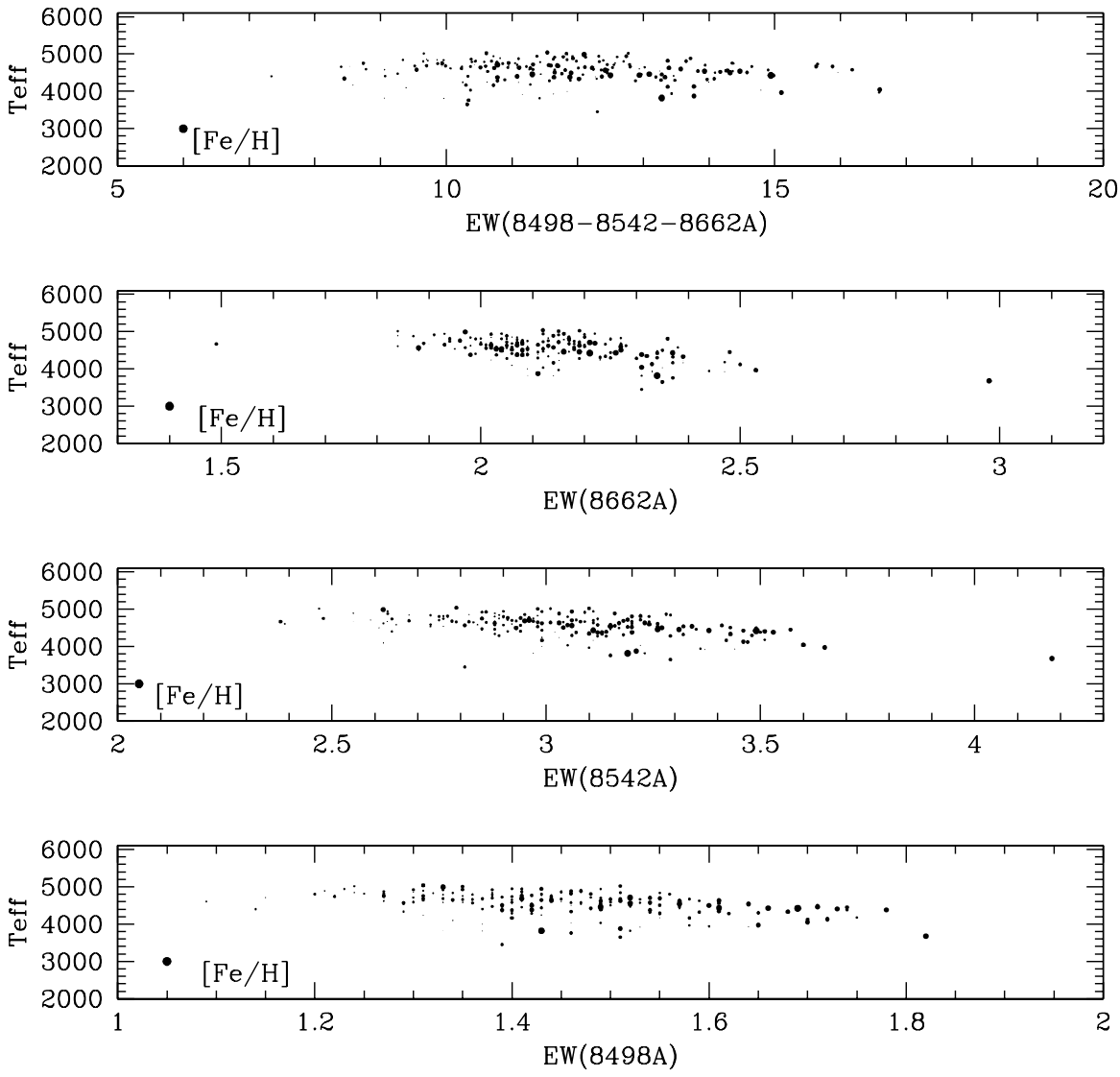

Fig. 4. Relation between the pseudo-equivalent widths in Angstroms and the effective temperature for the Ca II triplet lines. The size of the symbols represents the metallicity of the objects.

TABLE 3

COEFFICIENTS OF THE LINEAR POLYNOMIALS [a]

Effective Temperature

L_1	L_2	L_3	a_{01}	a_{02}	a_{03}	a_{04}	a_{05}	a_{06}	a_{07}	$N_{\rm in}$	$N_{\rm out}$	$\sigma_{T_{\rm eff}}$
1	2	3	9270	860	−7130	−3075	−142	−535	5016	97	7	152
1	2	4	7064	6	132	−2654	828	543	962	90	14	141
1	2	5	3657	764	−268	658	114	−302	−196	94	10	155
1	2	6	3960	748	−642	887	143	−500	−65	90	14	130
1	2	7	5588	783	−1836	−43	−245	−45	126	92	10	155
1	3	4	9562	−838	−3121	−3078	666	−92	2020	93	11	149
1	3	5	7588	61	−2298	−1101	336	−191	900	93	11	135
1	3	6	17562	19	−7530	−7493	−588	292	4711	93	11	125
1	3	7	2131	−916	1412	371	1042	−50	−219	91	11	146
1	4	5	4693	1054	−4716	1924	1660	−1186	283	90	14	136
1	4	6	3250	175	−31	1838	487	−516	−652	89	15	125
1	4	7	4929	−355	−371	318	602	−56	−134	87	14	134
1	5	6	3055	246	327	1445	82	−330	−314	89	15	126
1	5	7	6066	964	−342	−216	−384	6	68	90	12	148
1	6	7	5098	534	227	−101	−436	14	30	87	15	128
2	3	4	9579	−8554	2458	1392	5492	409	−1533	98	6	154
2	3	5	11801	−7332	−4139	−458	4962	109	48	97	7	142
2	3	6	16817	−4473	−6771	−5103	1755	730	2943	96	8	127
2	3	7	4889	−7451	413	547	5190	−13	−411	94	8	140
2	4	5	3706	−1389	−1086	2097	2968	−1245	−662	94	10	153
2	4	6	2263	−2045	2447	2311	976	−154	−1633	94	10	156
2	4	7	1433	−5211	5695	435	528	267	510	92	10	157
2	5	7	3307	640	206	1337	39	−691	−210	94	10	155
2	5	7	4498	572	475	−30	−583	38	−3	92	10	156
2	6	7	4081	397	973	−6	−829	39	−18	91	11	158
3	4	5	7904	−2790	2513	−2299	−1188	1950	−406	112	14	150
3	4	6	11337	−3368	3466	−6765	−3384	4564	239	113	13	148
3	4	7	5946	−1705	−6518	686	5494	−396	−119	108	15	157
3	5	6	9529	−3096	2153	−6027	−1669	4542	−94	114	12	152
3	5	7	12354	−4609	−3838	131	2509	−120	7	113	10	168
3	6	7	17242	−6792	−6750	−198	3860	17	77	113	10	162
4	5	6	−542	2848	854	2354	−273	−1259	−231	178	19	175
4	5	7	1504	1726	801	225	−439	−106	−20	170	22	167
4	6	7	354	5031	939	80	−1650	−184	91	174	18	175
5	6	7	1098	2444	827	−30	−878	−72	117	179	13	193

Surface Gravities

L_1	L_2	L_3	a_{01}	a_{02}	a_{03}	a_{04}	a_{05}	a_{06}	a_{07}	$N_{\rm in}$	$N_{\rm out}$	$\sigma_{\log g}$
1	2	3	13.19	1.99	−13.97	−6.94	0.26	−1.47	8.92	108	7	0.24
1	2	4	5.57	1.69	−6.23	−0.74	0.56	−1.27	2.31	112	3	0.27
1	2	5	5.09	0.13	−2.79	−0.16	0.48	−0.04	−0.10	110	5	0.26
1	2	6	5.81	−1.00	−0.05	−0.93	0.22	0.55	−0.99	110	5	0.25
1	2	7	6.91	1.18	−7.23	−0.18	0.31	−0.08	0.34	108	5	0.26
1	3	4	13.99	−0.14	−7.06	−7.95	0.19	0.10	4.51	106	9	0.23

TABLE 3 (CONTINUED)

Surface Gravities

L_1	L_2	L_3	a_{01}	a_{02}	a_{03}	a_{04}	a_{05}	a_{06}	a_{07}	$N_{\rm in}$	$N_{\rm out}$	$\sigma_{\log\, g}$
1	3	5	11.11	−1.17	−4.15	−2.70	0.48	0.23	1.12	113	2	0.30
1	3	6	25.22	−1.44	−11.64	−11.40	−0.37	0.95	5.88	109	6	0.24
1	3	7	−7.21	−1.27	7.56	1.00	0.99	0.00	−0.79	109	4	0.30
1	4	5	3.50	0.24	0.77	−0.62	−0.80	0.38	−0.20	106	9	0.23
1	4	6	7.96	0.27	−2.94	−2.25	−0.12	0.06	0.94	110	5	0.26
1	4	7	4.90	0.32	−2.25	−0.05	0.00	0.00	0.05	104	9	0.22
1	5	6	10.57	−1.31	−0.64	−3.78	0.02	0.64	0.22	110	5	0.26
1	5	7	10.60	0.26	−3.25	−0.44	0.15	−0.04	0.17	110	3	0.29
1	6	7	15.51	0.56	−6.59	−0.85	−0.09	−0.02	0.42	108	5	0.24
2	3	4	17.99	−18.52	−6.69	−0.63	10.60	3.72	−3.22	112	3	0.30
2	3	5	21.27	−17.40	−8.93	−1.97	9.25	1.68	−0.26	111	4	0.29
2	3	6	37.54	−5.42	−17.69	−17.95	−1.99	3.78	9.37	109	6	0.25
2	3	7	4.63	−13.35	0.41	0.91	8.31	0.15	−0.83	104	9	0.24
2	4	5	5.16	−1.18	−3.48	0.81	2.14	−0.56	−0.10	109	6	0.27
2	4	6	9.39	−2.93	−3.19	−1.72	1.61	0.33	0.35	112	3	0.28
2	4	7	7.71	−3.42	−3.98	0.04	2.37	0.00	0.00	106	7	0.25
2	5	6	7.83	−7.94	1.43	−1.81	0.56	2.73	−0.87	112	3	0.28
2	5	7	10.21	−1.69	−3.10	−0.23	0.98	−0.12	0.12	105	8	0.25
2	6	7	15.41	2.10	−6.87	−0.88	−0.42	−0.09	0.47	106	7	0.23
3	4	5	15.24	−6.45	−4.52	−3.25	1.36	1.56	0.72	135	2	0.31
3	4	6	32.43	−12.60	−1.32	−18.65	−4.65	9.19	3.62	127	10	0.24
3	4	7	15.33	−6.95	−17.60	0.78	11.29	−0.76	0.15	126	8	0.26
3	5	6	33.13	−15.24	0.62	−19.32	−2.40	10.64	1.28	132	5	0.26
3	5	7	15.58	−4.44	−7.62	0.30	3.95	−0.61	0.16	122	12	0.23
3	6	7	18.32	−4.27	−9.96	−0.24	3.88	−0.33	0.31	129	5	0.26
4	5	6	3.82	−3.10	1.20	−0.12	0.13	0.72	−0.49	196	15	0.24
4	5	7	3.88	5.58	−1.63	−0.35	−1.09	−0.24	0.23	188	17	0.23
4	6	7	8.40	3.57	−3.66	−0.57	−1.09	−0.12	0.35	187	18	0.22
5	6	7	9.00	0.90	−2.27	−0.71	−0.71	0.04	0.26	194	11	0.25

Metallicities

L_1	L_2	L_3	a_{01}	a_{02}	a_{03}	a_{04}	a_{05}	a_{06}	a_{07}	$N_{\rm in}$	$N_{\rm out}$	$\sigma_{[Fe/H]}$
1	2	3	−3.59	0.70	2.99	1.08	−0.62	0.20	−1.20	98	17	0.08
1	2	4	−1.69	1.00	0.97	−0.42	−0.66	−0.01	0.42	99	16	0.09
1	2	5	−1.71	1.14	0.65	−0.18	−0.65	−0.06	0.29	99	16	0.09
1	2	6	−0.59	1.33	−0.50	−0.80	−0.64	−0.17	0.96	99	16	0.09
1	2	7	−2.06	0.94	1.56	−0.03	−0.70	−0.01	0.01	97	16	0.08
1	3	4	−8.32	0.29	4.06	6.71	0.72	−0.70	−3.78	106	9	0.11
1	3	5	−5.31	0.61	2.00	2.01	0.44	−0.31	−0.98	104	11	0.11
1	3	6	0.20	0.00	−2.38	0.76	1.01	−0.50	0.25	101	14	0.10
1	3	7	1.71	−1.05	−2.10	0.05	1.13	−0.02	0.00	108	45	0.14
1	4	5	−0.88	1.56	−1.42	−0.11	−0.13	−0.38	0.64	104	11	0.11
1	4	6	−0.10	1.72	−1.61	−0.90	−0.42	−0.43	1.26	102	13	0.10
1	4	7	−2.92	1.34	1.61	−0.01	−0.69	−0.01	0.01	102	11	0.11
1	5	6	−0.86	1.82	−0.46	−0.75	−0.28	−0.34	0.51	99	16	0.09

TABLE 3 (CONTINUED)

Metallicities

L_1	L_2	L_3	a_{01}	a_{02}	a_{03}	a_{04}	a_{05}	a_{06}	a_{07}	$N_{\rm in}$	$N_{\rm out}$	$\sigma_{[Fe/H]}$
1	5	7	−3.52	1.18	1.06	0.05	−0.34	0.01	−0.02	101	12	0.10
1	6	7	−4.35	1.22	2.06	0.08	−0.59	0.02	−0.06	101	12	0.10
2	3	4	−5.90	0.07	1.57	6.12	2.34	−1.78	−2.98	107	8	0.13
2	3	5	−9.34	0.35	3.68	4.11	2.62	−1.03	−2.19	108	7	0.13
2	3	6	−6.55	−2.62	3.03	5.24	3.92	−0.81	−3.40	108	7	0.14
2	3	7	−0.54	−0.89	−1.34	0.26	2.20	−0.11	−0.10	105	8	0.13
2	4	5	−1.64	5.75	−2.85	−0.08	−0.65	−1.42	1.24	109	6	0.14
2	4	6	−0.29	5.27	−0.47	−2.52	−2.69	−0.38	1.84	107	8	0.13
2	4	7	−1.55	5.22	−0.71	−0.23	−1.98	−0.15	0.27	107	6	0.14
2	5	6	−1.64	2.25	2.01	−2.87	−1.75	1.68	0.16	107	8	0.13
2	5	7	−3.70	4.28	0.72	−0.04	−0.96	−0.06	0.04	106	7	0.13
2	6	7	−2.51	3.50	0.27	−0.01	−0.86	−0.08	0.05	105	8	0.13
3	4	5	−5.81	1.73	−1.76	3.58	3.17	−2.06	−0.59	126	11	0.14
3	4	6	−3.96	2.33	−2.62	3.48	2.84	−2.87	−0.04	128	9	0.15
3	4	7	1.02	−2.40	−0.52	0.04	1.43	0.04 *	−0.06	128	6	0.16
3	5	6	−3.09	1.78	0.25	1.18	0.21	−1.15	−0.03	122	15	0.13
3	5	7	−4.16	1.40	1.50	0.08	−0.62	0.05	−0.04	120	14	0.14
3	6	7	−3.48	0.75	1.66	0.12	−0.51	0.05	−0.07	126	8	0.16
4	5	6	−2.23	2.06	0.55	−0.48	−0.40	−0.19	0.15	190	21	0.12
4	5	7	−3.46	2.70	0.71	−0.02	−0.60	−0.03	0.02	190	15	0.13
4	6	7	−2.86	3.62	0.46	−0.10	−1.13	−0.03	0.07	192	13	0.14
5	6	7	−3.06	0.99	0.81	0.50	−0.29	0.01	0.02	187	18	0.13

[a]Involving all possible combinations for the three fundamental atmospheric parameters.

4.3. *Metallicities*

Figures 3 and 4 show the same correlations indicated in Figs. 1 and 2, but here the size of the points represents different metallicities in the giant star sample. The large points represent metal-rich stars and the small points metal-poor stars. It is observed for all the correlations that the metal-rich stars tend to be separated from the metal-poor ones. The behavior observed agrees with that indicated in Figure 5 of Cenarro et al. (2002), where a linear dependence of the Ca II triplet on the metallicity is found for giant stars. The range in metal abundances covers $-0.83 \leq$ [Fe/H] ≤ 0.53. The best fitting that recovers the metallicity is generated by a first order polynomial having the form

$$\begin{aligned}[Fe/H] = &-3.59 + 0.70 * EW_1 + 2.99 * EW_2 \\ &+ 1.08 * EW_3 - 0.62 * EW_1 * EW_2 \\ &+ 0.20 * EW_1 * EW_3 - 1.20 * EW_2 * EW_3 \ ,\end{aligned}$$

where EW_1, EW_2, and EW_3 correspond to the combinations 1 2 3 and the residual attains a value of 0.08 dex. The range of the residuals of [Fe/H] obtained for the linear solutions when we use one, two, and three independent variables has values of $\sigma[Fe/H] = 0.14 - 0.17$ dex, $\sigma[Fe/H] = 0.08 - 0.16$ dex, $\sigma[Fe/H] = 0.08 - 0.16$ dex, while using least-squares solutions we find $\sigma[Fe/H] = 0.11 - 0.18$ dex, $\sigma[Fe/H] = 0.08 - 0.16$ dex, $\sigma[Fe/H] = 0.08 - 0.16$ dex, respectively.

5. CONCLUSIONS

In the light of the results obtained, we can conclude that in the giant star sample studied the Na I doublet, a blend at 6497 Å, the Balmer Hα line and the Ca II triplet are sensitive to the three fundamental atmospheric parameters within the complete range of effective temperature, which agrees with Cenarro et al. (2002). It is also important to remark that for all the applied polynomials the residuals improve with the increase of the number of independent variables, and they are found to be practically independent from the order of the fitting for orders higher than one (linear). In the future, the inclusion of dwarf stars as well as the extension of the spectral type range could improve the calibrations for the determination of the fundamental atmospheric parameters.

The authors are deeply thankful to Decanato de Investigación of The Universidad Nacional Experimental del Táchira for the financial support given to this work.

REFERENCES

Alloin, D., & Bica, E. 1989, A&A, 217, 57
Carter, D., Visvanathan, N., & Pickles, A. J. 1986, ApJ, 311, 637
Cenarro, A. J., Cardiel, N., Gorgas, J., Peletier, R. F., Vazdekis, A., & Prada, F. 2001, MNRAS, 326, 959
Cenarro, A. J., Gorgas, J., Cardiel, N., Pedraz, S., Peletier, R. F., & Vazdekis, A. 2001, MNRAS, 326, 981
Cenarro, A. J., Gorgas, J., Cardiel, N., Vazdekis, A., & Peletier, R. F. 2002, MNRAS, 329, 863
Díaz, A. I., Terlevich, E., & Terlevich, R. 1989, MNRAS, 239, 325
Jones, J. E., Alloin, D. M., & Jones, B. J. .T. 1984, ApJ, 283, 457
Mallik, S. V. 1994, A&AS, 124, 359
Malyuto, V., & Schmitd-Kaler, Th. 1999, in ASP Conf. Ser. Vol. 167, Harmonizing Cosmic Distance Scales in a Post-Hipparcos Era, eds. D. Egret & A. Heck (San Francisco: ASP)
Stock, J., & Stock, M. J. 1999, RevMexAA, 35, 143
Valdes, F., Gupta, R., Rose, J. A., Singh, H., & Bell, D. 2004, ApJS, 152, 251V
Vazdekis, A., Cenarro, A. J., Gorgas, J., Cardiel, N., & Peletier, R. F. 2003, MNRAS, 340, 1317
Weaver, B., & Torres-Dodgen, A. V. 1995, ApJ, 446, 300
Worthey, G., Faber, S. M., González, J. J., & Burstein, D. 1994, ApJS, 94, 687
Zhou, X. 1991, A&A, 248, 367

Ramón Molina: Universidad Nal. Experimental del Táchira, UNET, Decanato de Investigación, Coordinación de Ciencias Exactas y Naturales, Av. Universidad, Paramillo, San Cristóbal, Táchira 5001, Venezuela (rmolina@unet.edu.ve).
Jürgen Stock: Centro de Investigaciones de Astronomía, CIDA, Av. Alberto Carnevalli, Sector "La Hechicera", Mérida, Venezuela.